PHYSICAL REVIEW A VOLUME 22, NUMBER 2 AUGUST 1980

Electron capture by heavy multicharged ions from atomic hydrogen at low velocities

D. H. Crandall, R. A. Phaneuf, and F. W. Meyer
Oak Ridge National Laboratory, Oak Ridge, Tennessee 37830
(Received 10 March 1980)

Total cross sections for capture of an electron by Xe^{q+} ($2 \leq q \leq 12$), Ar^{q+} ($2 \leq q \leq 9$), and Fe^{q+} ($q = 5,6$) colliding with atomic and molecular hydrogen have been measured for velocities between 10^7 and 10^8 cm/s. The cross sections vary from below 1×10^{-16} cm^2 to just above 100×10^{-16} cm^2, with the measured values for $q \geq 4$ all greater than 37×10^{-16} cm^2. The cross sections are independent of ionic species for a given q and are generally constant with changing velocity. The cross sections increase linearly with q up to $q = 9$, but for the highest-charge states $q = 9$–12, the data suggest that the cross sections do not continue to increase as rapidly with increasing q.

I. INTRODUCTION

Electron capture by multicharged ions has received considerable attention recently. Motivation for this research activity derives from both basic physics and applications. The large cross sections, dependence of cross sections on ionic charge, and dominance of capture into excited states provide new tests of our fundamental understanding of the electron-transfer process. In addition, multicharged ions occur in the plasmas of fusion research and astrophysics and have significant effect on the character and evolution of these plasmas. Since capture is the largest inelastic cross section for these ions at low and intermediate velocities, it is generally important in physical environments where they occur.

The present paper is concerned with electron transfer during collisions in which the velocity is significantly less than the orbital velocity of the electron that is captured (Bohr orbit, $v_0 = 2 \times 10^8$ cm/s). In this low-velocity region, our previously measured total capture cross sections[1] have not accurately followed the generalized scaling rules[2] for variation of cross section with ionic charge or velocity. Our previous measurements were for light ions of B, C, N, and O which had only a few electrons remaining on the incident ion. The present measurements are for heavier, partially stripped ions of Xe, Fe, and Ar which retain significantly more electrons, resulting in some change in the character of the cross sections.

In the low-velocity region, a quasimolecular concept is generally accepted as appropriate for describing the collision. The energy levels of the active electron in this quasimolecule can be calculated for simple systems, and the collisionally induced transitions between these molecular energy levels can be calculated in various approximations. Theoretical calculations based on this approach have had some success predicting measured cross sections[1,2] but are not reasonably applied to collision systems which have many electrons. In such cases with many electrons the number of molecular potential curves and their interactions is large, and additional approximations can be made, usually leading to generalized results dependent on the initial ionic charge, the initial binding energy of the active electron, and the collision velocity.[3–8] The available experimental results at low velocities for collision systems with many electrons are for multielectron targets,[9–15] and those experimental results have been able to distinguish which of the predicted scalings of cross section versus initial ionic charge and target electron binding energy are most appropriate for multielectron target cases.[16,17] The present measurements test scalings for the important atomic-hydrogen case in which a large number of electrons are present only on the incident ion. In addition, the scaling of cross section with ionic charge is tested for higher charges than in any of the previous low-velocity experiments. Details of the scaling of cross sections derived from present data are presented in Sec. III.

II. EXPERIMENTAL TECHNIQUE

The measurements were performed with the same apparatus and procedures described in Ref. 1. Ions are extracted from a Penning Ion Gauge (PIG)-type source and analyzed by crossed magnetic and electric fields to select ions of a given mass-to-charge ratio (m/q). These ions are passed through a thin-walled tungsten cell which contains target gas and which can be heated to sufficient temperatures to dissociate 92% of the molecular hydrogen (by passing current directly through the tungsten). Immediately after the tungsten cell, an electrostatic deflector is used to separate the ion beam into its charge-state components so that the electron-capture cross section can be determined.

A. Uncertainties associated with ion beam

Some of the experimental difficulties associated with the ion beam were more thoroughly investigated for the present data than for the data of Ref. 1. Ion-beam identification was aided by increased dispersion and by more precise control and monitoring of the magnetic field of the purifying magnet, which is located just before the tungsten cell and well isolated from the many ion source parameters and m/q selection fields. The field of the purifying magnet could be measured and reset to better than ±0.2%, and the scaling of the measured magnetic field required to transmit ions of different m/q and acceleration voltage followed the calculated scaling to about ±0.5%.

Ion-beam purity was found to be a significant problem in some of the present measurements. Electron capture provides a direct method of estimating ion-beam purities even for cases with identical m/q of the incident ions.[18,19] Relative intensities of the ion-beam components can be estimated if the capture cross sections are known for the different ion-beam components in any given target gas. In the present case the following beam contaminant problems were encountered and corrected for: $^{40}Ar^{5+}$ contaminated by 5% of $^{16}O^{2+}$, $^{40}Ar^{8+}$ contaminated by 4% of $^{10}B^{2+}$, $^{56}Fe^{6+}$ contaminated by strongly variable amounts of $^{28}Si^{3+}$ (the Si^{3+} component was undetectable, ≤2% for data reported here), and $^{56}Fe^{6+}$ contaminated by traces of $^{64}Cu^{7+}$ (Cu^{7+} was eliminated by careful control of ion source parameters and m/q selector). In addition, we found that the following ion beams were uncontrollably contaminated so that measurements of capture cross sections could not be made: Fe^{2+} contaminated by N_2^+ and CO^+, Fe^{3+} contaminated by Xe^{7+}, Fe^{4+} contaminated by N^+, Fe^{7+} contaminated by Ar^{5+} and O^{2+}, Fe^{8+} contaminated by N^{2+}, and Fe^{9+} contaminated by several other beams of nearly the same m/q. In general production of Fe^{q+} beams presented difficulty. Fe was introduced into the source discharge as iron pentacarbonyl $Fe(CO)_5$ and a small amount of either Xe or Ar gas was found to be essential to maintain source discharge and sputter-clean the cathodes. Thus contaminants of C, O, Ar, or Xe, as well as the always present N ions, could not be eliminated. However, pure beams of Fe^{5+} and Fe^{6+} were obtained.

Our previously reported cross sections for Ar^{8+} (Ref. 1) were found to be incorrect, probably due to undetected contamination by B^{2+}. We have rechecked many of our published measurements, and this is the only case found to be in error. Since a beam contaminant of this type contributes to the measured number of incident ions N_i, but does not contribute to the electron capture signal N_c, the cross sections deduced from

$$\sigma_{q,q-1} = (N_c/N_i)/t$$

(where t is target thickness) will be artifically low if undetected contaminants are present. Our previously reported cross sections for Ar^{8+} in H_2 and H are found to be too low by about 50%. Those previous measurements with Ar^{8+} were conducted immediately after measurements with B^{q+} ions. The B^{2+} contaminant was not specifically searched for in the earlier measurements with Ar^{8+} and the BF_3 gas used is known to contaminate the ion source for several days after its use.

The ion-beam transmission optics before the charge-purifying magnet were used in a strongly focusing mode for the present measurements, and careful tuning was necessary to insure that the ion beam was significantly smaller than the channeltron active area at the point of detection. This was verified by sweeping the primary or charge-transfer components across the detector with the deflecting plates, or by fixing the deflecting voltage and translating the detector across the beam. A steeply rising, flat-topped response indicated total ion-beam collection.

The question of ion-beam stability and its effect on measured cross sections was tested in the present experiments. For both the experiments described in Ref. 1 and the present work, a single detector was used to detect the incident ions and the electron-capture ions, by means of programming the voltage on the final electrostatic analyzer to select which ion-beam component was incident on the detector. Typically, the primary beam was examined for 1 s, and the electron-capture component for 5 or 10 s. The switching cycle was carried out for 10 repeats to produce one trial of a cross-section (or background) measurement. A computer controlled timing, beam switching, and counter gating. Beam-intensity fluctuations on time scales of a few seconds could thus influence a measurement. For the data of Ref. 1 the relative uncertainties reported were counting statistics only and were sufficiently large to mask fluctuations in cross-section measurements due to beam-intensity fluctuations. For the present data more time was spent on each data point and counting statistics were reduced to a low level [usually less than ±1% standard deviation (s.d.)]. Also, for these present results every cross-section trial was repeated several times (generally four to ten repeats), both with gas in the tungsten cell and with gas bypassing the cell but injected into the vacuum chamber. The relative uncertainties given in the tables are derived from statistical analysis of the repeated trials, not from counting statistics. Thus

TABLE I. Summary of experimental uncertainties (in percentage).

Source	$\sigma_{q,q-1}(H)$	$\sigma_{q,q-1}(H_2)$
Typical statistical reproducibility (90% confidence level)	5	5
Uncertainty ascribed to cross sections used for normalization	10	10
Other systematic uncertainties		
Ion-beam purity (effect on σ)	2	2
Beam collection and counting efficiency	3	3
Target-gas purity (effect on σ)	3	6
Reproducibility of target-thickness calibration (90% confidence level)	4.5	3.1
Measurement of relative target-gas flow	1	1
Uncertainty in dissociation fraction	4	
Typical quadrature sum	13.6	13.6

the presently quoted statistical uncertainties represent reproducibility of measurements which is affected by counting statistics and any of the other variables which could change between trials, which we believe are dominated by short-term ion-beam-intensity fluctuations. Nevertheless, the reproducibility given in the tables are generally better than ±5% at 90% confidence level.

B. Uncertainties associated with the gas target

The techniques for handling target gas and procedures for determining target density are identical to those previously described.[1,20] We use the gas bypass technique of Bayfield[21] so that the same amount of gas enters the vacuum system whether it enters the gas cell during a cross-section trial or bypasses the gas cell during a background trial. The relative amount of gas entering the vacuum system is determined by measurement of the pressure drop across a standard external copper tube, through which all target gas is required to pass. The conductance of the copper tube is much lower than that of the gas cell. This pressure drop can be reproducibly measured to better than ±1% with a capacitance manometer for the gas flows used during the experiments. At the end of the present series of measurements, the target thickness (particle density times cell length) was independently calibrated for hot- and cold-target conditions by normalization to the known cross sections for $H^+ + H^0 \rightarrow H^0 + H^+$ at 20 keV for a hot target and to $H^+ + H_2 \rightarrow H^0 + (\text{all products})^+$ at 20 keV for a cold target, as described in Refs. 1 and 20. In addition, the relative stability of this calibration was tested during the several months of the present data acquisition by measurements of the cross section for $N^{4+} + H\,(\text{and } H_2) \rightarrow N^{3+} + (\text{products})^+$ at 40 keV (repeated on 16 different days). The variability of the average of this measurement is 4.5% at 90% confidence level for the atomic-hydrogen target and 3.1% at 90% confidence level for the molecular-hydrogen target, as reflected in Table I for the "reproducibility of calibration."

The total experimental uncertainties are tabulated in Table I. A typical data point has a total absolute uncertainty of about ±14% (quadrature sum of statistical reproducibility at 90% confidence level, all systematic uncertainties, and uncertainty ascribed to the cross sections used as standards for calibration). Systematic uncertainties have been estimated at a high confidence intended to be equivalent to 90% confidence level on statistics.

III. RESULTS AND DISCUSSION

All of the measured cross sections and statistical uncertainties are given in Table II. The general character of the cross sections is illustrated in Fig. 1, which shows the data for $Xe^{q+} + H$ and $Ar^{q+} + H$. The data for the lowest-charge states Ar^{2+}, Xe^{2+}, and Xe^{3+} are decreasing abruptly with decreasing velocity and are well separated from cross sections for more highly charged ions. This behavior of Ar^{2+}, Xe^{2+}, and Xe^{3+} is typical of nonresonant-capture cross sections between singly charged ions and neutral atoms, which peak strongly for collision velocities approximately equal to the orbital velocity of the captured electron, and for which capture is usually favored only between atomic ground states. For $q \geq 4$ the measured cross sections are all large and independent of velocity in the range currently tested. This behavior is typical of multicharged ions,[2,11] at least for cases where many electrons are involved. For highly charged ions, capture is usually favored to

TABLE II. Measured electron-transfer cross sections for multicharged ions in H and H_2.

Ion	Laboratory energy (keV)	Velocity (10^7 cm/s)	$\sigma_{q,q-1}$(H) (10^{-16} cm^2)	$\sigma_{q,q-1}$(H_2) (10^{-16} cm^2)
Xe^{2+}	6.3	0.96	0.64(0.38)[a]	17.6(0.3)
Xe^{2+}	20.4	1.73	1.71(0.34)	15.6(0.3)
Xe^{3+}	9.1	1.16	0.92(0.19)	2.25(0.21)
Xe^{3+}	16.0	1.53	1.56(0.23)	2.90(0.21)
Xe^{3+}	30.6	2.12	2.34(0.38)	4.93(0.17)
Xe^{3+}	60.6	2.99	7.22(0.11)	22.4(0.6)
Xe^{4+}	12.0	1.33	53.1(2.1)	33.9(0.8)
Xe^{4+}	21.3	1.77	44.2(1.3)	27.6(0.9)
Xe^{4+}	40.8	2.45	46.7(2.3)	24.2(0.8)
Xe^{4+}	80.8	3.45	53.6(0.9)	30.2(1.5)
Xe^{5+}	15.3	1.50	43.9(3.4)	30.4(2.5)
Xe^{5+}	26.7	1.98	44.7(1.5)	32.3(0.6)
Xe^{5+}	51.0	2.71	47.0(1.5)	32.1(1.9)
Xe^{5+}	101	3.86	46.6(1.1)	35.1(0.9)
Xe^{5+}	132	4.41	42.6(1.9)	34.8(1.3)
Xe^{6+}	18.3	1.64	56.9(2.7)	31.4(1.1)
Xe^{6+}	32.0	2.17	54.9(3.2)	31.2(0.8)
Xe^{6+}	61.2	2.97	50.8(2.5)	28.5(0.6)
Xe^{6+}	121	4.22	57.3(2.5)	34.7(1.7)
Xe^{6+}	156	4.79	56.6(2.8)	54.9(4.0)
Xe^{7+}	21.5	1.78	68.0(3.4)	49.3(2.3)
Xe^{7+}	37.3	2.34	70.8(2.1)	52.5(1.3)
Xe^{7+}	71.4	3.21	62.8(3.8)	47.5(3.2)
Xe^{7+}	141	4.56	77.4(3.6)	47.8(2.3)
Xe^{7+}	182	5.18	73.2(3.8)	52.2(2.7)
Xe^{8+}	24.0	1.88	76.3(2.4)	57.9(1.0)
Xe^{8+}	42.6	2.51	65.8(1.8)	53.8(1.6)
Xe^{8+}	81.6	3.43	77.9(3.4)	55.8(0.6)
Xe^{8+}	162	4.88	76.5(2.8)	53.2(1.4)
Xe^{8+}	208	5.54	71.1(3.6)	51.6(1.8)
Xe^{9+}	27.0	1.99	93.2(3.1)	69.4(0.8)
Xe^{9+}	48.0	2.66	87.8(5.0)	63.9(2.1)
Xe^{9+}	91.8	3.64	95.3(9.2)	72.0(4.3)
Xe^{9+}	182	5.18	81.6(4.8)	65.5(1.2)
Xe^{9+}	234	5.87	79.6(7.8)	75.0(1.9)
Xe^{10+}	30.0	2.10	102.7(1.9)	79.8(4.0)
Xe^{10+}	53.3	2.80	97.8(7.4)	69.8(4.0)
Xe^{10+}	102	3.83	88.2(8.2)	72.7(1.3)
Xe^{10+}	202	5.46	79.0(4.4)	68.6(1.4)
Xe^{10+}	261	6.19	92.0(6.2)	72.6(2.1)
Xe^{11+}	110	4.03	95.8(8.4)	83.5(1.9)
Xe^{11+}	222	5.72	104.0(7.7)	83.7(5.7)
Xe^{12+}	121	4.21	81.0(5.3)	59.1(8.2)
Xe^{12+}	242	5.98	71.2(8.5)	59.7(5.3)
Fe^{5+}	17.6	2.46	49.6(2.9)	35.7(1.9)
Fe^{5+}	26.2	3.00	51.4(2.5)	32.6(1.2)
Fe^{5+}	51.0	4.19	49.4(1.4)	30.4(0.7)
Fe^{5+}	65.2	4.74	46.9(2.5)	30.1(1.9)
Fe^{5+}	75.2	5.09	46.4(2.2)	29.8(1.0)
Fe^{5+}	102.3	5.94	45.6(2.2)	28.8(0.9)
Fe^{6+}	21.0	2.69	48.9(3.5)	43.3(1.8)
Fe^{6+}	31.6	3.30	58.1(1.8)	43.0(0.7)
Fe^{6+}	45.2	3.95	53.5(2.0)	46.9(0.9)
Fe^{6+}	60.9	4.57	55.6(1.8)	45.0(1.0)
Fe^{6+}	78.5	5.20	57.2(5.1)	38.5(2.5)
Fe^{6+}	124.2	6.54	50.7(2.8)	41.5(2.0)
Ar^{2+}	10.5	2.26	1.40(0.30)	1.84(0.15)

TABLE II. *(Continued.)*

Ion	Laboratory energy (keV)	Velocity (10^7 cm/s)	$\sigma_{q,q-1}$(H) (10^{-16} cm^2)	$\sigma_{q,q-1}$(H_2) (10^{-16} cm^2)
Ar^{2+}	25.2	3.49	2.44(0.23)	3.21(0.30)
Ar^{2+}	44.2	4.62	3.40(0.36)	3.81(0.25)
Ar^{3+}	15.8	2.76	28.3(1.1)	12.2(0.4)
Ar^{3+}	37.6	4.26	24.3(2.3)	13.4(1.0)
Ar^{3+}	66.3	5.66	25.4(1.4)	15.7(0.9)
Ar^{4+}	21.1	3.19	38.4(2.3)	32.7(0.8)
Ar^{4+}	50.1	4.92	39.4(0.9)	29.8(0.9)
Ar^{4+}	88.4	6.53	36.8(2.1)	30.7(0.9)
Ar^{5+}	26.4	3.57	43.8(1.7)	31.9(1.2)
Ar^{5+}	62.7	5.50	44.6(1.7)	34.2(1.1)
Ar^{5+}	110	7.30	45.5(1.7)	36.0(1.3)
Ar^{6+}	31.7	3.91	51.1(3.9)	38.2(0.9)
Ar^{6+}	75.5	6.04	49.7(3.4)	39.3(1.6)
Ar^{6+}	133	8.00	53.2(3.1)	37.6(1.6)
Ar^{7+}	37.0	4.23	72.0(2.8)	53.5(1.1)
Ar^{7+}	87.9	6.51	64.7(2.0)	49.6(1.2)
Ar^{7+}	155	8.64	59.7(2.0)	45.9(2.0)
Ar^{8+}	42.2	4.51	67.7(4.7)	62.9(1.8)
Ar^{8+}	101	6.97	62.1(4.8)	57.1(1.9)
Ar^{8+}	177	9.24	62.4(2.0)	55.3(0.9)
Ar^{9+}	55.7	5.18	78.6(4.9)	62.2(4.2)
Ar^{9+}	114	7.41	75.6(4.8)	55.9(2.1)
Ar^{9+}	199	9.80	67.0(5.7)	56.6(3.4)

[a] Numbers in parentheses are statistical reproducibility at 90% confidence level.

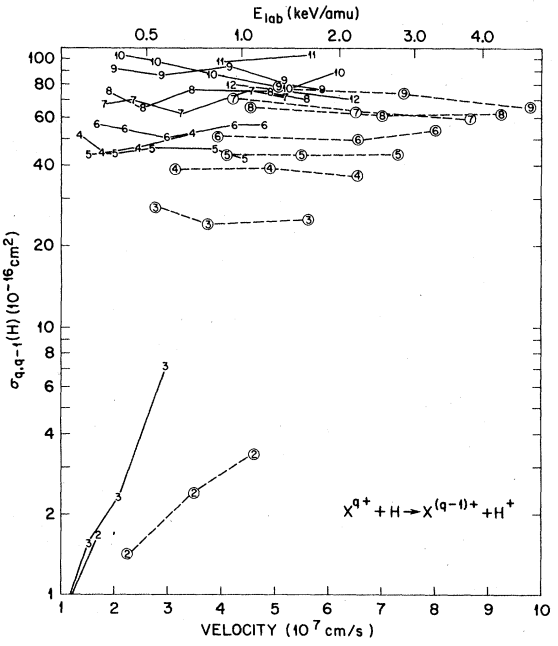

FIG. 1. Electron-capture cross sections for Ar^{q+} and Xe^{q+} in atomic H. Numbers indicate initial charge state q. Circles numbers connected by dashed lines are Ar^{q+}, and numbers connected by solid lines are Xe^{q+}. Relative uncertainties at 90% confidence level are typically the same size as the circles.

several excited states of the final ion. It is also seen in Fig. 1 that for $5 \leq q \leq 9$ there is no distinguishable difference in the cross sections for the Ar and Xe ions (the Fe^{5+} and Fe^{6+} data were not plotted on Fig. 1 because they lie on top of the other $q = 5$, 6 data points).

Figure 2 shows atomic-hydrogen cross sections for $q = 4$–6 at 4×10^7 cm/s from the present measurements and from the previous data,[1] plotted as a function of the number of electrons remaining on the incident ion. An interesting trend is exhibited in that for a given ionic charge those ions with few electrons remaining have distinctly lower cross sections than the heavy, many-electron ions. The cases with few electrons are qualitatively similar to the one-electron diatomic-molecule cases which have been calculated in coupled-state approximations[2,8,22–30] where only a few avoided curve crossings of the molecular stationary states determine the cross sections. For these cases the cross sections often decrease with decreasing velocity from 2 to 0.2×10^8 cm/s.

For the many-electron ions the picture is qualitatively more like the generalized models which have been calculated assuming many curve crossings[3,4] or a generalized motion (tunneling) of the electron in the average field of the colliding system.[5,6] In the many-electron case the cross sec-

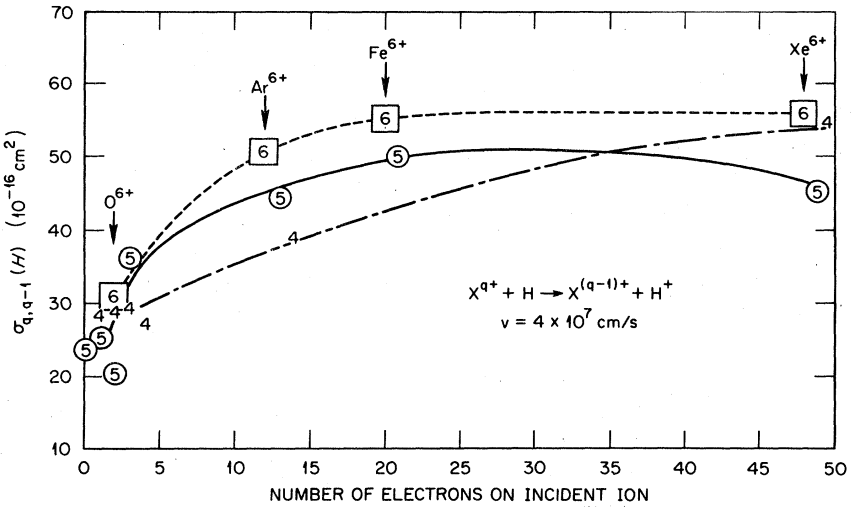

FIG. 2. Measured electron-capture cross sections in atomic H for ions of initial charge $q = 4$–6 as a function of the number of electrons attached to the incident ion. For fewer than five attached electrons, the data are from Ref. 1. Remaining cases are present data.

tions have little variation with changing velocity in the 2 to 0.2×10^8 cm/s range. Thus, the cross sections for many-electron cases might be expected to be slightly higher than for the few-electron cases at 4×10^7 cm/s velocity, as observed.

In Ref. 1 it was argued that, for electron capture, a number of multielectron systems might behave like the more accurately calculable one-electron diatomic-molecule cases. Within narrow velocity limits this was demonstrated for $(OH)^{6+}$ compared to $(CH)^{6+}$, $(NH)^{5+}$ compared to $(BH)^{5+}$, and $(CH)^{4+}$ compared to $(BeH)^{4+}$. However, the present data imply that many-electron ions do not, in general, have cross sections the same as the one-electron case of the same charge. Figure 3 shows present data for Ar^{8+} and Xe^{8+} compared to the several published theoretical results for O^{8+}, all with atomic-hydrogen target. At the highest velocity tested, the Ar^{8+} and Xe^{8+} results lie within the extremes of the calculations, but at the lowest velocity the theories are uniformly about a factor of three lower than the present data. Of course, it remains to be proven experimentally that at low velocities the O^{8+} cross section follows the theory rather than the present many-electron data. However, Figs. 2 and 3 are consistent in suggesting that at low velocity the many-electron ions usually have higher cross sections than the nearly fully stripped ions of the same charge and velocity.

Comparison of the present data with measurements using multielectron targets show that the character of cross sections with the atomic-hydrogen target is not qualitatively different from data with other atomic species as targets. A recent study by Müller *et al.*[17] demonstrated the

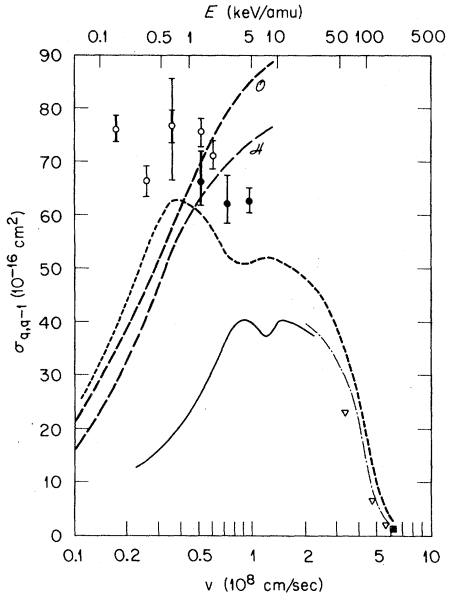

FIG. 3. Electron-capture cross sections in atomic H for ions of initial charge $q = 8$. Open circles are present data for Xe^{8+}, closed circles are present data for Ar^{8+}, open triangles are experiment for Fe^{8+} from Ref. 35, and solid square is experiment for O^{8+} from Ref. 35. Theories are represented by curves and are all for O^{8+}: Short-dashed curve is unitarized distorted-wave approximation of Ref. 26, solid curve is two-coupled-state calculation of Ref. 22, dot-dashed curve is classical theory of Ref. 25, long-dashed curves are eight-state-perturbed-stationary-state results for atomic orbitals expanded on H and O nuclei (as indicated) from Ref. 25. Error bars on present data are 90% confidence level on statistical reproducibility except that the outer bar on the point at 0.34×10^8 cm/s is total absolute uncertainty at high confidence.

scaling of capture cross sections as a function of the ionization potential of neutral atom targets. Figure 4 shows present data for Xe^{10+} incident on H, H_2, and He as well as those of Müller *et al.* for a variety of multielectron targets all at $v = 3.8 \times 10^7$ cm/s. The present data are lower than those of Müller *et al.* but follow the predicted scaling with ionization potential. As seen, the data follow most closely the scaling (ionization potential)$^{-2}$, predicted by Presnyakov and Ulantsev.[3] From the present data we have 68 cases for $q \geq 4$ in which we can compare the cross sections for the H_2 and the H targets for a given ion and velocity. The ratio $R = \sigma(H)/\sigma(H_2)$ is found to be 1.36 ± 0.02 (s.d. of mean). This is a remarkably stable ratio and is very close to the inverse square scaling with target ionization potential, which predicts $R = 1.32$.

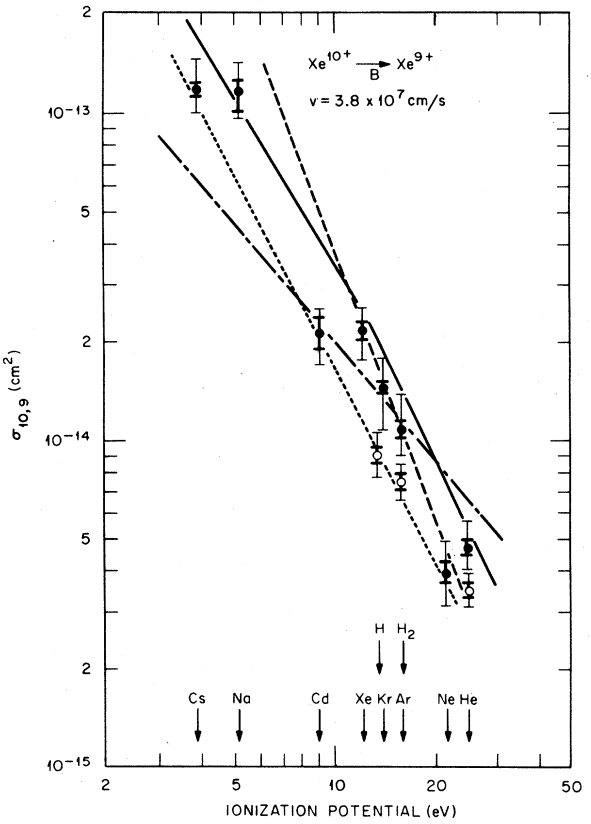

FIG. 4. Electron capture for Xe^{10+} in various gases at 3.8×10^7 cm/s as a function of ionization potential of the target gas. Present data are open circles with inner error bars for statistical reproducibility at 90% confidence level and outer bars for absolute uncertainty at high confidence. Solid circles are data of Müller *et al.* (Ref. 17) with inner and outer error bars of the same meaning but at 67% confidence level. Theories are represented by curves: Solid curve is from Grozdanov and Janev (Ref. 6), short-dashed curve is from Presnyakov and Ulantsev (Ref. 3), and dot-dashed curve is from Olson and Salop (Ref. 4). The long-dashed curve is scaling deduced from other experimental values (Ref. 16).

TABLE III. Comparison of present cross sections for He and Ar targets with those of Müller, Salzborn *et al.*

Ion	Lab energy (keV)	Present $\sigma_{q,q-1}$(He) (10^{-16} cm^2)	Müller $\sigma_{q,q-1}$(He) (10^{-16} cm^2)	Ratio Müller to present
Xe^{6+}	61.2	16.1(0.8)	21.5	1.34
Xe^{7+}	71.4	24.6(0.7)	26.5	1.08
Xe^{10+}	100	34.3(1.4)	46.0[a]	1.34
		$\sigma_{q,q-1}$(Ar)	$\sigma_{q,q-1}$(Ar)	
Xe^{6+}	61.2	30.6(1.0)	42.4	1.38
Xe^{7+}	71.4	52.8(2.1)	69.0	1.31

Average ratio = 1.29 ± 0.05 s.d.

[a] This value from Ref. 17, all other values of Müller *et al.* were obtained from Ref. 10 by interpolating or extrapolating from measurements at energies slightly different from those of the present measurements which are given in the table.

We have measured cross sections for a few specific ions with He and Ar targets specifically to compare with results of Müller, Salzborn *et al.* Table III shows the comparison. Müller *et al.* state that their absolute uncertainty is ±25% [10,17] (presumably at 67% confidence level corresponding to one s.d. on statistics). Since our present data are uncertain by ±14% (at high confidence intended to correspond to 90% confidence level), the quadrature sum of the quoted experimental uncertainties is 29%—equal to the average discrepancy between the sets of data of Table III. The discrepancy is qualitatively the same as observed earlier[9,31] for Ar^{q+} + Ar capture cross sections.

The most interesting scaling of present cross-section data is with initial ionic charge. Figure 5 shows calculated cross sections compared with present data for Ar^{q+} and Xe^{q+} at 4×10^7 cm/s, all for the atomic-hydrogen target. This scaling has recently been discussed by a number of authors (see Refs. 2 and 11 for examples), and a linear scaling of $\sigma_{q,q-1}$ with q is generally accepted. Experimental data for q up to 8 and for nonatomic-hydrogen target were analyzed by Müller and Salzborn,[16] who found $\sigma \propto q^{1.17}$ as the best fit. Ryufuku and Watanabe have made a best fit to their unitarized distorted-wave calculations for the atomic-hydrogen target and find $\sigma \propto q^{1.06}$ as a best fit.[32] The two theories plotted on Fig. 5 give approximately $\sigma \propto q$. The present data (while uniformly lower than the generalized theories) show the expected scaling quite reliably up through $q = 9$.

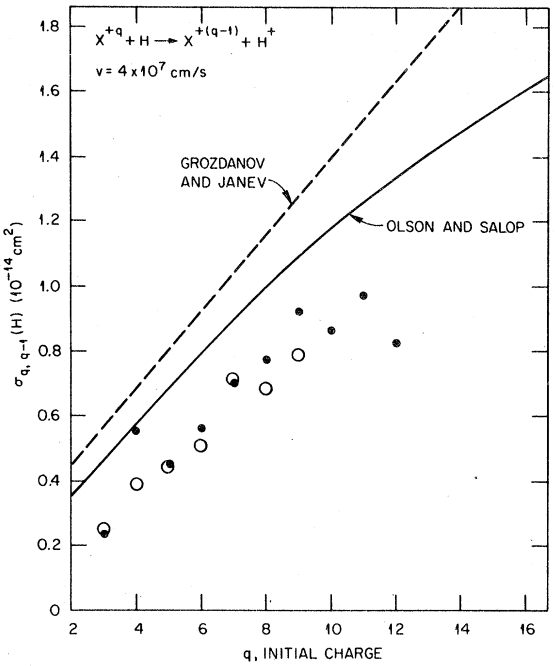

FIG. 5. Electron capture for ions in atomic H as a function of initial ionic charge q at 4×10^7 cm/s. Open circles are present data for Xe^{q+} and solid circles are for Ar^{q+}. Dashed curve is from Grozdanov and Janev (Ref. 6), and solid curve is from Olson and Salop (Ref. 4).

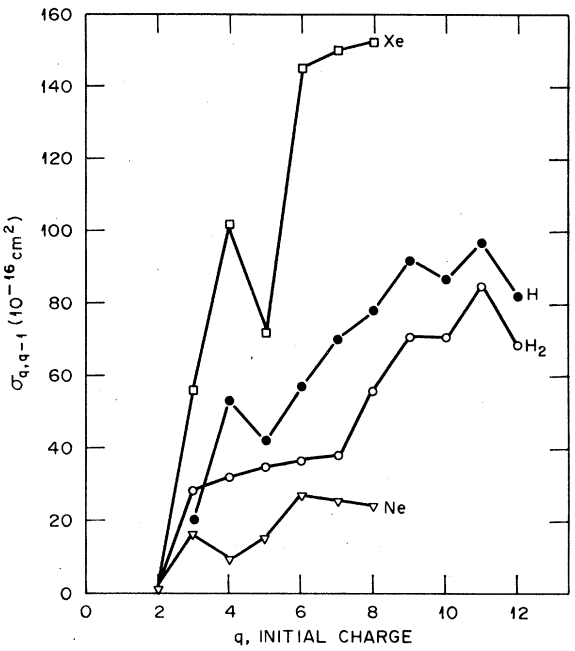

FIG. 6. Electron capture for ions of Xe^{q+} in H, H_2, Xe, and Ne as a function of initial ionic charge q. Data for H and H_2 targets are present results for $v = 4 \times 10^7$ cm/s, and data for Xe and Ne targets are from Müller (Ref. 10) for $v = 2 \times 10^7$ cm/s.

There are only three data points for $q > 9$ and although the scatter prevents a definitive statement, these data suggest that, for higher q, the cross sections increase less than linearly with q.

Figure 6 shows data for Xe^{q+} for various targets at low velocity. The suggestion of less-than-linear scaling in $\sigma_{q,q-1}$ vs q is apparent in all cases. Of course, the experimental data do not include multiple-electron capture (for multielectron targets), capture of electrons into the continuum,[33,34] or capture into doubly excited states which autoionize before charge analysis. At high velocities, near 4×10^8 cm/s, the scaling of $\sigma_{q,q-1}$ vs q is significantly different but generally follows a power of q at a given velocity. However, for heavy ions distinct oscillation about this power-law behavior has been observed[35,36] and qualitatively may be associated with capture into autoionizing states.[37] The present suggested departure from linear scaling at low velocity may be a manifestation of this same process. The measurements at high velocity show slow oscillation of σ vs q for $q = 6$–15 with Ta^{q+} ions on H. If the present departure from $\sigma \propto q$ represents the same effect, measurements at higher q should show completion of an oscillation in σ vs q.

Clearly the question of σ vs q scaling should remain a point of investigation. It is an important issue for applied as well as basic considerations. For example, in the fusion program it is important to have accurate estimates of the production of protons in collisions such as $Fe^{21+} + H$ in order to model the energy deposition of injected neutral beams used to heat fusion plasma. The present results suggest that generalized theories may overestimate the electron-transfer cross sections for high-q ions in atomic hydrogen.

ACKNOWLEDGMENTS

The authors are indebted to J. A. Hale for continuing technical assistance and to C. F. Barnett for encouragement and supportive discussions. The research was sponsored by the Offices of Basic Energy Sciences and Magnetic Fusion Energy of the U. S. Department of Energy under Contract No. W-7405-eng-26 with the Union Carbide Corporation.

[1]D. H. Crandall, R. A. Phaneuf, and F. W. Meyer, Phys. Rev. A 19, 504 (1979).
[2]R. E. Olson, in *Electronic and Atomic Collisions*, edited by N. Oda and K. Takayanagi (North-Holland, Amsterdam, 1980), p. 391.
[3]L. P. Presnyakov and A. D. Ulantsev, Kvantovaya Electron. Moscow 1, 2377 (1974) [Sov. J. Quant. Electron. 4, 1320 (1975)].
[4]R. E. Olson and A. Salop, Phys. Rev. A 14, 579 (1976).
[5]M. I. Chibisov, Zh. Eksp. Teor. Fiz. Pis'ma Red. 21, (1976) [JETP Lett. 24, 46 (1976)].
[6]T. P. Grozdanov and R. K. Janev, Phys. Rev. A 17, 880 (1978).
[7]V. P. Shevelko, Z. Phys. A 287, 19 (1978).
[8]H. Ryufuku and T. Watanabe, Phys. Rev. A 19, 1538 (1979).
[9]H. Klinger, A. Müller, and E. Salzborn, J. Phys. B 8, 230 (1975). See also E. Salzborn, IEEE Trans Nucl. Sci. NS-23, 947 (1976).
[10]A. Müller, thesis, Giessen, West Germany (unpublished).
[11]E. Salzborn and A. Müller, in *Electronic and Atomic Collisions*, edited by N. Oda and K. Takayanagi (North-Holland, Amsterdam, 1980), p. 407.
[12]D. H. Crandall, M. L. Mallory, and D. C. Kocher, Phys. Rev. A 15, 61 (1977).
[13]D. H. Crandall, Phys. Rev. A 16, 958 (1977).
[14]L. D. Gardner, J. E. Bayfield, I. A. Sellin, D. J. Pegg, R. S. Peterson, M. L. Mallory, and D. H. Crandall, Phys. Rev. A 20, 766 (1979).
[15]B. A. Huber, H. J. Kahlert, H. Schrey, and K. Wiesemann, in *Abstracts of Contributed Papers of the XI International Conference on the Physics of Electronic and Atomic Collisions*, edited by K. Takayanagi and N. Oda (Kyoto, Japan, 1979), p. 582.
[16]A. Müller and E. Salzborn, Phys. Lett. 62A, 391 (1977).
[17]A. Müller, C. Achenbach, and E. Salzborn, Phys. Lett. 70A, 410 (1979).
[18]M. L. Mallory and D. H. Crandall, IEEE Trans. Nucl. Sci. NS-23, 1069 (1976).
[19]D. H. Crandall, R. A. Phaneuf, and P. O. Taylor, Phys. Rev. A 18, 1911 (1978).
[20]R. A. Phaneuf, F. W. Meyer, and R. H. McKnight, Phys. Rev. A 17, 534 (1978).
[21]J. E. Bayfield, Phys. Rev. 182, 116 (1969).
[22]C. Harel and A. Salin, J. Phys. B 10, L213 (1977).
[23]A. Salop and R. E. Olson, Phys. Rev. A 16, 1811 (1977).
[24]J. Vaaben and J. S. Briggs, J. Phys. B 10, L512 (1977).
[25]A. Salop and R. E. Olson, Phys. Rev. A 19, 1921 (1979).
[26]H. Ryufuku and T. Watanabe, Phys. Rev. A 18, 2005 (1978).
[27]A. Salop and R. E. Olson, Phys. Lett. A71, 407 (1979).
[28]R. E. Olson, E. J. Shipsey, and J. C. Browne, J. Phys. B 11, 699 (1978).
[29]E. J. Shipsey, J. C. Browne, and R. E. Olson (private communication).
[30]T. A. Green, E. J. Shipsey, and J. C. Browne (private communication).
[31]D. H. Crandall, M. L. Mallory, and D. C. Kocher, Phys. Rev. A 15, 61 (1977).
[32]H. Ryufuku and T. Watanabe (private communication). This scaling, $\sigma \propto q^{1.06}$, is a slight modification of the value given by these authors in Ref. 8, which was $\sigma \propto q^{1.12}$.
[33]R. Shakeshaft, Phys. Rev. A 18, 1930 (1978).
[34]C. R. Vane, I. A. Sellin, S. B. Elston, M. Suter, R. S. Thoe, G. D. Alton, S. D. Berry, and G. A. Glass, Phys. Rev. Lett. 43, 1388 (1979).
[35]F. W. Meyer, R. A. Phaneuf, H. J. Kim, P. Hvelplund, and P. H. Stelson, Phys. Rev. A 19, 515 (1979).
[36]H. J. Kim, P. Hvelplund, F. W. Meyer, R. A. Phaneuf, P. H. Stelson, and C. Bottcher, Phys. Rev. Lett. 40, 1635 (1978).
[37]C. Bottcher, in *Coherence and Correlation in Atomic Collisions*, edited by H. Kleinpoppen and J. F. Williams (Plenum, New York, 1980), p. 403.